p-ISSN 2089 – 0133 e-ISSN 2477-6416
URL : https://jurnal.uns.ac.id/ijap/article/view/106868

DOI : https://doi.org/10.13057/ijap.v16i1.106868

# APPLICATION OF 1D MAGNETOTELLURIC METHOD TO ESTIMATE ALLUVIUM THICKNESS IN ACEH RIVER DELTA

**Fajrul Hani[1,2], Nazli Ismail[1,2]*, Muhammad Syukri Surbakti[1], Fadhli Syamsuddin[1], Amir Asyqari[1], Muhammad Nanda[3], Badrul Munir[2], Muhammad Arfan Alhafsi[2], Tomi Afrizal[4]**

[1]Department of Physics, Faculty of Mathematics and Natural Sciences, Universitas Syiah Kuala, Indonesia
[2]Department of Geophysical Engineering, Faculty of Engineering, Universitas Syiah Kuala, Indonesia
[3]Department of Marine Sciences, Faculty of Marine and Fisheries, Universitas Syiah Kuala, Indonesia
[4]Graduate School of Mathematics and Applied Sciences, Universitas Syiah Kuala, Indonesia
*nazli.ismail@usk.ac.id

Received 2025-10-22, Revised 2026-04-23, Accepted 2026-04-28,
Available Online, Published Regularly June 2026

## ABSTRACT

The Aceh River Delta, located in Banda Aceh City and Aceh Besar Regency, is a Quaternary alluvial plain composed of unconsolidated young sediments and lies between two northern branches of the Great Sumatran Fault, making it vulnerable to earthquake amplification and liquefaction. Estimating the thickness of alluvium is essential for seismic risk assessment. This study applies the 1D magnetotelluric (MT) method to investigate subsurface resistivity and estimate alluvium thickness. MT data were acquired in Cot Seunong Village using a KMS-820 data logger, LEMI-120 magnetometer, and LEMI-701 electrodes for 14 hours. Processing included time-frequency analysis, notch filtering, and robust transfer function estimation using the EMTF algorithm. Apparent resistivity and phase data were inverted using IPI2WIN to produce a 1D resistivity model. The model reveals seven subsurface layers to 1000 m depth, with the upper six layers (0–420 m) having low to moderate resistivity (13.9–134.9 Ωm), interpreted as alluvium. The deepest layer (914.2 Ωm) likely represents sandstone-conglomerate bedrock. The model correlates well with nearby borehole lithology. These findings confirm the effectiveness of the 1D MT method in estimating alluvium thickness and detecting resistivity contrasts. The estimated alluvium thickness of 420 m increases vulnerability to seismic wave amplification at the ground surface. Further surveys using 2D/3D MT inversion are recommended to provide comprehensive information on vertically and laterally subsurface conditions, thereby enhancing geohazard assessment in the Aceh River Delta.

Keywords: Aceh River Delta; Alluvium thickness; 1D Magnetotelluric method; Resistivity; Sedimentary

## INTRODUCTION

The Aceh River Delta is a low-lying area located at the northern tip of Sumatra Island and covers the administrative areas of Banda Aceh City and Aceh Besar Regency, Indonesia. As a densely populated urban area that serves as the economic center of Aceh Province, this region plays an important role in regional development. In a geological context, the delta lies between the two northernmost branches of the Great Sumatran Fault (GSF) and is underlain by young alluvium deposits formed by river and coastal sedimentation [1]. Areas with unconsolidated sediments and active tectonics, such as this delta, are vulnerable to amplified ground shaking and liquefaction during an earthquake [2], which can cause infrastructure damage and disrupt various vital community activities [3]. Therefore, in-depth studies are needed to obtain information about the thickness of alluvium sediments, particularly as part of efforts to reduce earthquake risk in the Aceh River Delta.

Copyright © 2026 Universitas Sebelas Maret

Geophysical studies are reliable for investigating subsurface structures, with efficiency, low cost, and environmental friendliness advantages. In studies to estimate sediment thickness, which requires deep penetration, the most suitable geophysical method is magnetotellurics [4]. The magnetotelluric method is a passive electromagnetic method that measures variations in electric and magnetic fields originating from nature in the low-frequency range of $10^{-4}$ Hz to $10^{4}$ Hz [5]. The application of magnetotelluric methods has been widely used for various studies, such as oil and gas exploration [6], geothermal [7], groundwater resources [8], mineral resources [9], regional geological structures [10], and lithospheric tectonic studies [11]. This method has also been successfully applied to studies of alluvium sediment thickness. For example, the application of the magnetotelluric method has successfully estimated the thickness of alluvium sediments in the Kachchh Basin, India, with results of 700–800 m [12]. Similar studies have been conducted in the northern Indo-Gangetic plain [13] and the alluvial plains of the central Ganga Basin, India [14].

The effectiveness of the magnetotelluric method in estimating the thickness of alluvium sediments in various other regions forms the basis for applying this method in our research in the Aceh River Delta. Although several researchers have studied alluvium deposits in this region, they have used different methods with limited depth penetration. For example, research by [15] utilized borehole data and reported the presence of alluvium sediments to a depth of 206 m in Cot Paya village, located downstream from the region. In a subsequent study [16] employed a shallow shear wave reflection technique to assess the Aceh River Delta sediment thickness, with up to 100 m investigations. Research by [1] utilized borehole data in conjunction with the vertical electrical sounding (VES) method to elucidate the sedimentation processes within the Aceh River Delta, particularly concerning its interconnection with groundwater resources. In general, their studies covered investigations to a depth of ±200 m. Due to the relatively shallow investigation depth, their research could not show the boundary between the alluvium formation and the underlying rock formation to accurately estimate the thickness of alluvium sediments in the Aceh River Delta.

This study used the 1D magnetotelluric method, which offers the advantage of investigating deeper depths. This study is an initial stage in applying the magnetotelluric method to estimate alluvium thickness in the Aceh River Delta. Previous studies have used the magnetotelluric method for other purposes, such as assessing the existence of the Great Sumatran Fault (GSF) [17-18] and for geothermal studies [19-20]. However, no studies have used the magnetotelluric method to estimate the thickness of alluvium sediments in this region. The study area proximity to the urban area of Banda Aceh poses significant challenges in applying the magnetotelluric method, which is sensitive to artificial electrical disturbances. To overcome this challenge, the data acquisition point was strategically placed in locations less affected by noise and adjacent to a borehole site. This approach is intended to facilitate correlation between the 1D resistivity model results and borehole data from previous studies [1].

Based on these considerations, this study aims to estimate the thickness of alluvium sediments in the Aceh River Delta using the 1D magnetotelluric method. The results serve as a foundation for more comprehensive follow-up studies using the magnetotelluric method, including expanding the survey area and improving data resolution to provide a more detailed image of the subsurface structure, both laterally and vertically. Additionally, the findings assist local governments in assessing and enhancing earthquake disaster mitigation policies in the Aceh River Delta.

Copyright © 2026 Universitas Sebelas Maret

## GEOLOGICAL AND TECTONIC SETTING

Geologically (Figure 1), the Aceh River Delta consists mainly of young alluvium deposits, comprising gravels, sands, silts, clays, and marine sediments [21-22]. Most of these sediments were deposited along the Aceh River during the Quaternary period [1]. The rock formations exposed on the Aceh Fault ridge in the southwest consist of carbonate rocks formed during the Jurassic to Cretaceous periods as oceanic accretionary rocks. They belong to the Woyla group [21]. Volcanic rock formations consisting of andesite-tuff are found in the northeast of the delta. In the southeast, there are outcrops of tuffaceous sandstone and lithosol conglomerate dating from the Plio-Pleistocene [23].

Tectonically, the Aceh River Delta lies within the active Sumatra Fault zone, a dextral strike-slip fault approximately 1900 km long that has been active since the Middle Miocene due to the oblique subduction of the Indo-Australian Plate against the Eurasian Plate west of Sumatra Island [24]. This fault is segmented into 19 segments, with two main segments in the Aceh River Delta region: the Aceh Segment and the Seulimeum Segment. This fault zone has a high level of stress accumulation, as determined by seismological analysis, and is suspected to be capable of triggering large, destructive earthquakes [25]. Notable historical seismic events in this region include the Mw 6.5 earthquake in 1964 in the Seulimeum segment, the Mw 6.0 earthquake in 1997 in the Aceh segment [26], and the most recent seismic event in 2025 (Figure 1), namely the Mw 5.2 earthquake in the Seulimeum segment.

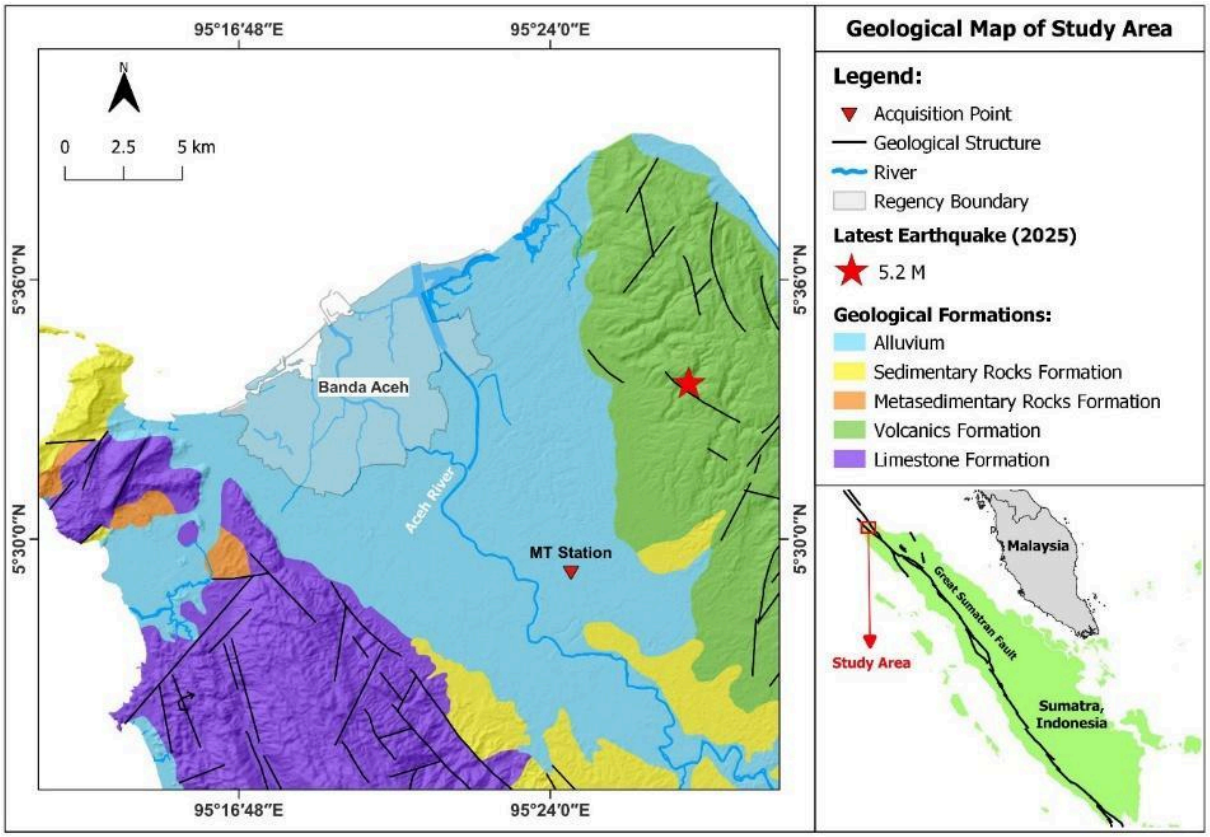



**Figure 1.** Geological map of the study area modified from [21]

Copyright © 2026 Universitas Sebelas Maret

## METHOD

### Basic Theory

The magnetotelluric (MT) method is a passive geophysical method that utilizes natural sources from natural electromagnetic fields to image subsurface characteristics. Various complex physical processes generate the electromagnetic field measured in the magnetotelluric method with a $10^{-4}$ Hz to $10^{4}$ Hz. At frequencies >1 Hz, it is caused by meteorological activity such as lightning. Lightning causes electromagnetic waves between the ionosphere and the Earth [27]. Meanwhile, frequencies <1 Hz come from the interaction between the solar wind and the Earth's magnetic field, which creates the magnetosphere [5].

In its practical application (Figure 2), the magnetotelluric method involves the simultaneous recording of magnitudes of time-varying electromagnetic field components, namely horizontal electric fields ($E_x$, $E_y$) and magnetic fields in both horizontal ($H_x$, $H_y$) and vertical ($H_z$) orientations. The $x$- and $y$-directions are defined as north-south and east-west, respectively.

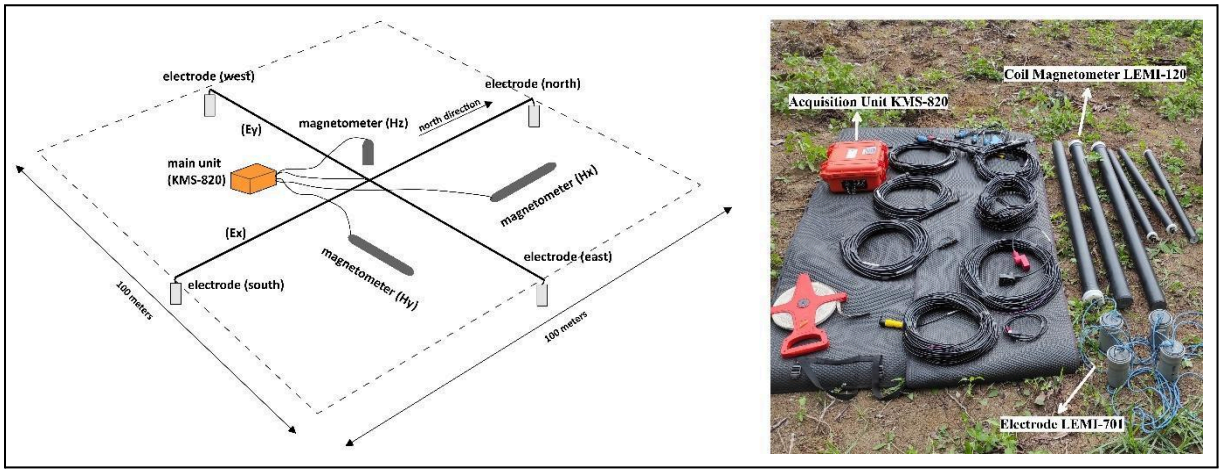



**Figure 2.** MT data acquisition scheme using KMS-820 data logger, LEMI-120 coil magnetometer, and LEMI-701 electrode

The electric field ($E$) and magnetic field ($H$) components in the frequency domain have a mathematical relationship in the form of an impedance tensor ($Z$). This impedance is a complex second-order matrix that relates the orthogonal components of the electric field ($E$) and magnetic field ($H$) [28]. In the case of 1D earth, it is assumed that there is no induced electric field parallel to the induced field [29]. Therefore, the impedance tensor ($Z$) equation can be written as:

$$\begin{bmatrix} E_x & E_y \end{bmatrix} = \begin{bmatrix} 0 & Z_{xy} \\ -Z_{yx} & 0 \end{bmatrix} \begin{bmatrix} H_x & H_y \end{bmatrix} \quad (1)$$

The tensor element ($Z_{ij}$) is used to obtain information about the variation of rock resistivity values in the subsurface. The apparent resistivity ($\rho_a$) and phase ($\Phi$) values can be extracted as transfer functions from the impedance tensor ($Z_{ij}$),

Copyright © 2026 Universitas Sebelas Maret

$$\rho_a = \frac{1}{\omega\mu_0}\left|Z_{ij}\right|^2 \quad (2)$$

and

$$\Phi = arctan\left(\frac{Im\left(Z_{ij}\right)}{Re\left(Z_{ij}\right)}\right) \quad (3)$$

Based on (2), the apparent resistivity is calculated from the values of the electric field (***E***) and magnetic field (***H***) in the frequency domain. Meanwhile, the phase angle difference between the electric field (***E***) and magnetic field (***H***) in (3) is theoretically 45°. According to [5], in the case of 1D magnetotellurics, a phase >45° indicates a conductor, while a phase <45° reflects a resistor at a certain depth.

In addition to the relationship between the electric field and the horizontal magnetic field components, magnetotelluric analysis in the frequency domain also incorporates the vertical magnetic field component ($H_z$) to enhance the interpretation of subsurface resistivity structures. The interaction between the horizontal magnetic components ($H_x$, $H_y$) and the vertical component ($H_z$) is described by a geomagnetic transfer function known as the tipper (***T)***. This relationship is mathematically expressed as,

$$H_z = T_{zx}H_x + T_{zy}H_y \quad (4)$$

where the tipper vector ($T_{ij}$) is a complex transfer function consisting of real and imaginary parts. Tipper can be used as a qualitative interpretation, where the real part of this vector can be visualized in the form of an induction arrow pointing toward the subsurface conductor [30].

### Acquisition and Processing of Magnetotelluric Data

Magnetotelluric data acquisition was conducted in September 2024 in Cot Seunong Village, Montasik District, Aceh Besar Regency. This village is located approximately 12 km southeast of Banda Aceh City (Figure 3a). The survey location is at an elevation of 20 m and is geomorphologically classified as an alluvial plain, as shown in Figure 3b, with the Barisan Mountains in the background. Magnetotelluric data were recorded over 14 hours using the KMS-820 instrument as the data logger and monitor unit, the LEMI-120 coil magnetometer to measure the magnetic field, and the LEMI-701 electrode to measure the electric field.

Copyright © 2026 Universitas Sebelas Maret

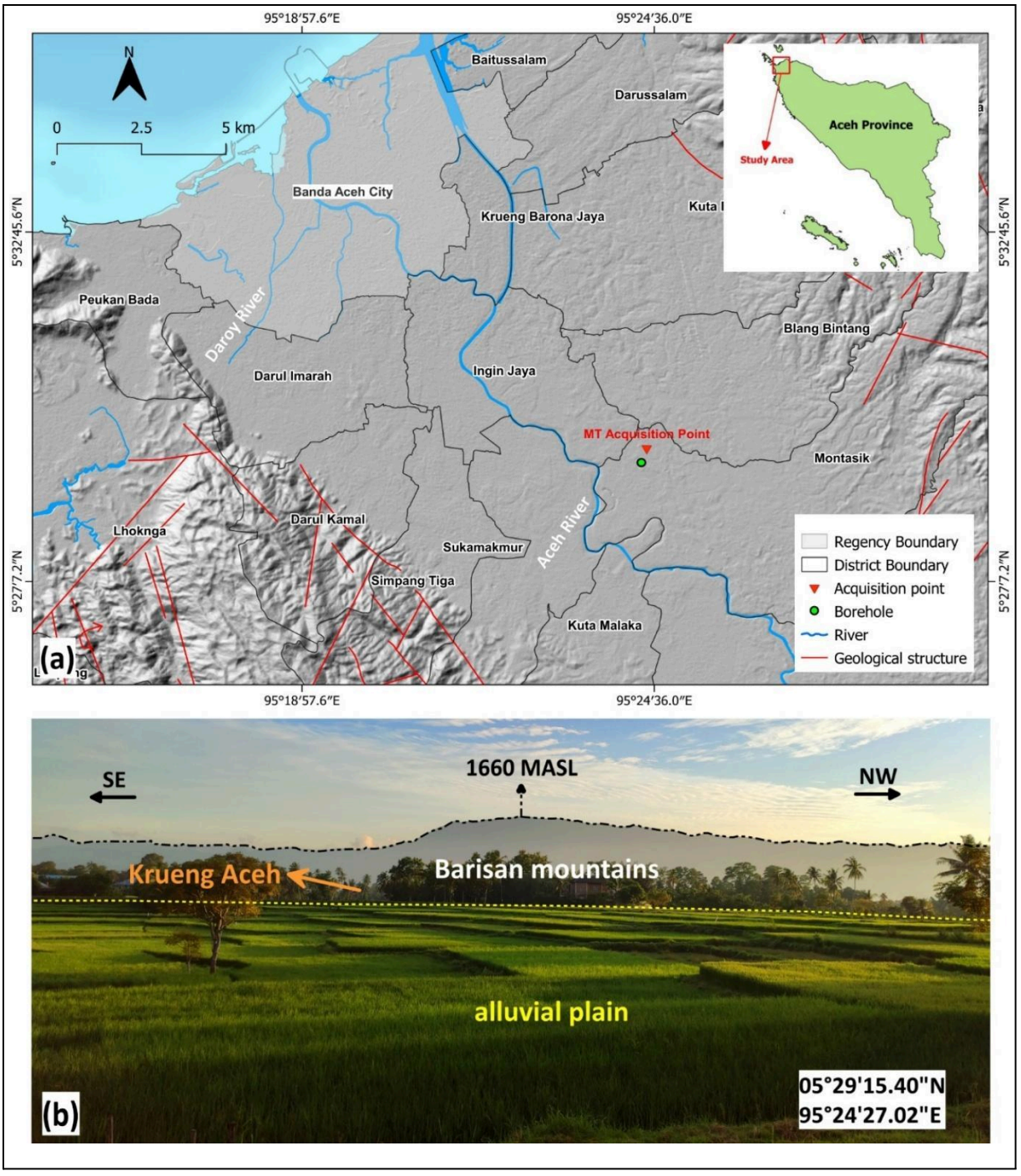



**Figure 3.** (a) Location of MT data acquisition and borehole; (b) Landform of the MT data acquisition area

Time series data were obtained from magnetotelluric measurements. This data consists of variations in the electric and magnetic fields. Advanced analysis was performed to inspect data quality, such as time-frequency analysis to identify noise sources and filtering techniques to reduce noise effects [31]. The noise-reduced time series data were used to calculate the transfer function using the KMS-820 processing software based on the EMTF algorithm developed by Oregon State University [32]. The EMTF algorithm processes the data through a fast Fourier transform (FFT) to convert the data from the time domain to the frequency domain and robust processing to reduce the influence of outliers, which are often considered residual noise from the data [33]. The output of the EMTF algorithm is an EDI file containing

Copyright © 2026 Universitas Sebelas Maret

impedance tensor and tipper information at each frequency.

The apparent resistivity and phase values can be calculated from the impedance tensor values using equations (2) and (3). These apparent resistivity and phase data are input files in the 1D inversion modeling process using IPI2WIN MT software to obtain a 1D resistivity model against depth. This 1D resistivity model forms the basis for subsurface geological interpretation.

## RESULT AND DISCUSSION

Figure 4 shows samples of time series data obtained in this study using a KMS-820 data acquisition unit with a sampling frequency of 1000 Hz. The time series data shown in Figure 4 shows a regular and correlated peak amplitude pattern in all MT data components. This peak amplitude pattern is likely caused by noise affecting data quality. The quality of EM method data generally depends heavily on the signal-to-noise ratio [34]. EM methods such as magnetotellurics, which utilize low-frequency natural signals, are susceptible to noise contamination, which can corrupt time series data and reduce the accuracy of transfer function calculations [35]. Therefore, it is important to evaluate the quality of data obtained from the field by identifying noise and determining the best techniques to reduce its influence.

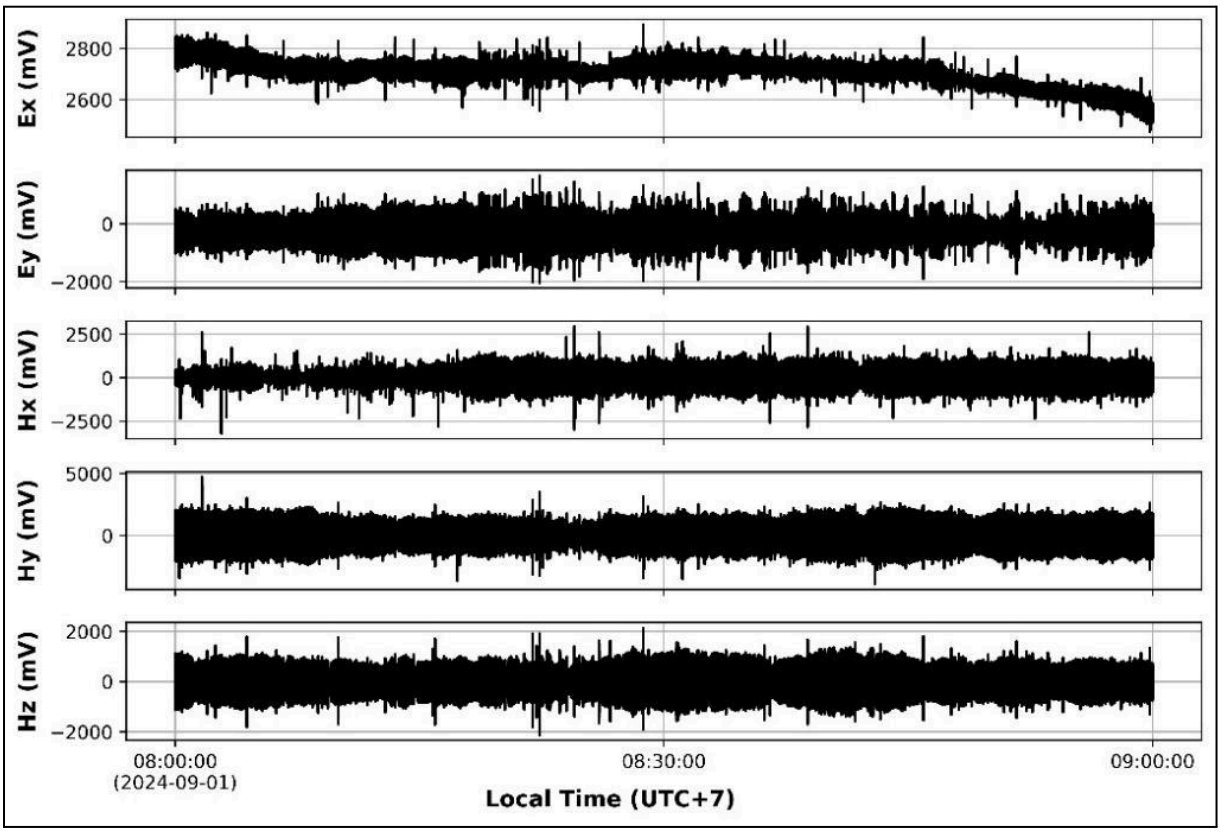



**Figure 4.** Samples of the time series data for all components ($E_x$, $E_y$, $H_x$, $H_y$, $H_z$) were displayed over one hour

Noise sources in time series data can be identified through time-frequency analysis by calculating the short-time Fourier transform (STFT) of the electric field components ($E_x$, $E_y$) and magnetic field components ($H_x$, $H_y$, $H_z$). The STFT is a computational technique that groups time-domain input signals (discrete signals) into segments and applies the FFT to each segment [36]. The STFT calculation is expressed by,

Copyright © 2026 Universitas Sebelas Maret

$$X_{STFT}(m,\ k) = \sum_{n=0}^{N-1} x(n\ +\ mH)w(n)e^{-j\frac{2\pi kn}{N}} \quad (5)$$

where $x(n)$ is the input signal, $N$ is the window length, $w(n)$ is the window function, $m$ is the time index in the segment, and $k$ is the frequency index. The $H$ symbol is the hop size, determining the displacement length between segments. The parameters used in the calculation can be seen in the following Table 1.

**Table 1.** Parameters and inputs for spectrogram calculation

| Parameters | Inputs |
|---|---|
| Window length | 1024 |
| Window function | Hanning window |
| Overlap (N-H) | 50% |

The result of the STFT calculation (5) for all MT data components is a spectrogram in units of power/frequency (dB/Hz) presented in Figure 5. Based on the figure, the highest power value (represented in yellow) is at a frequency of 50 Hz, which occurs continuously throughout the period, both for the electric and magnetic fields. Similar events can also be seen at the harmonic frequencies, 100 Hz to 450 Hz, with higher power occurring at odd number harmonics than even numbers. This indicates the presence of powerline noise around the acquisition area, affecting the MT data obtained.

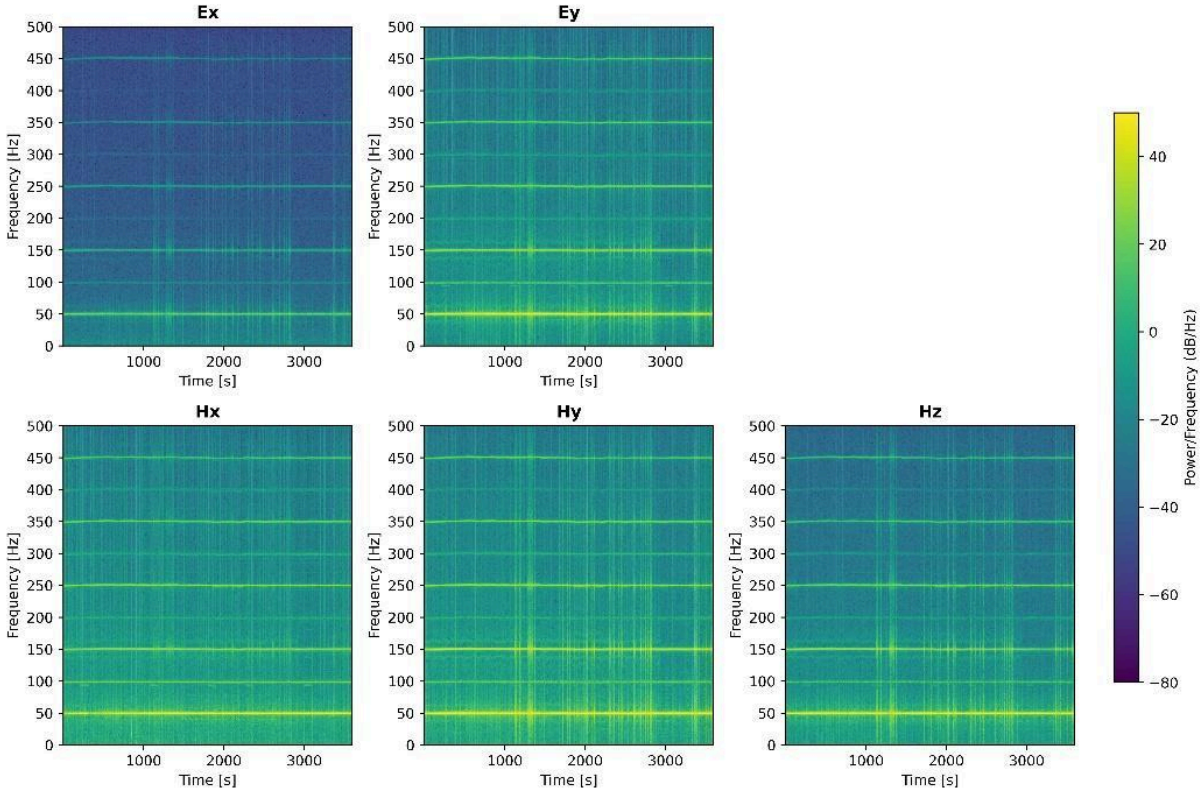



**Figure 5** Spectrogram for all components ($E_x$, $E_y$, $H_x$, $H_y$, $H_z$)

Powerline noise can be eliminated or reduced with a filtering technique called a notch filter [37]. The notch filter is a band-stop filter that rejects parts of the signal between the cut-off frequency or the frequency to be removed. It can be applied to one frequency and extended to

Copyright © 2026 Universitas Sebelas Maret

all its harmonics, so the notch filter technique is quite efficient for reducing the influence of powerline noise [38].

Figure 6 provides an example of the MT data condition in the frequency spectrum before and after applying the notch filter. In Figure 6a, the MT data in the frequency spectrum identified a spectral peak at 50 Hz and its harmonics. After filtering (Figure 6b), the spectral peak at 50 Hz and its harmonics are no longer visible. This proves that the notch filter technique is quite effective in reducing the influence of powerline noise on MT data.

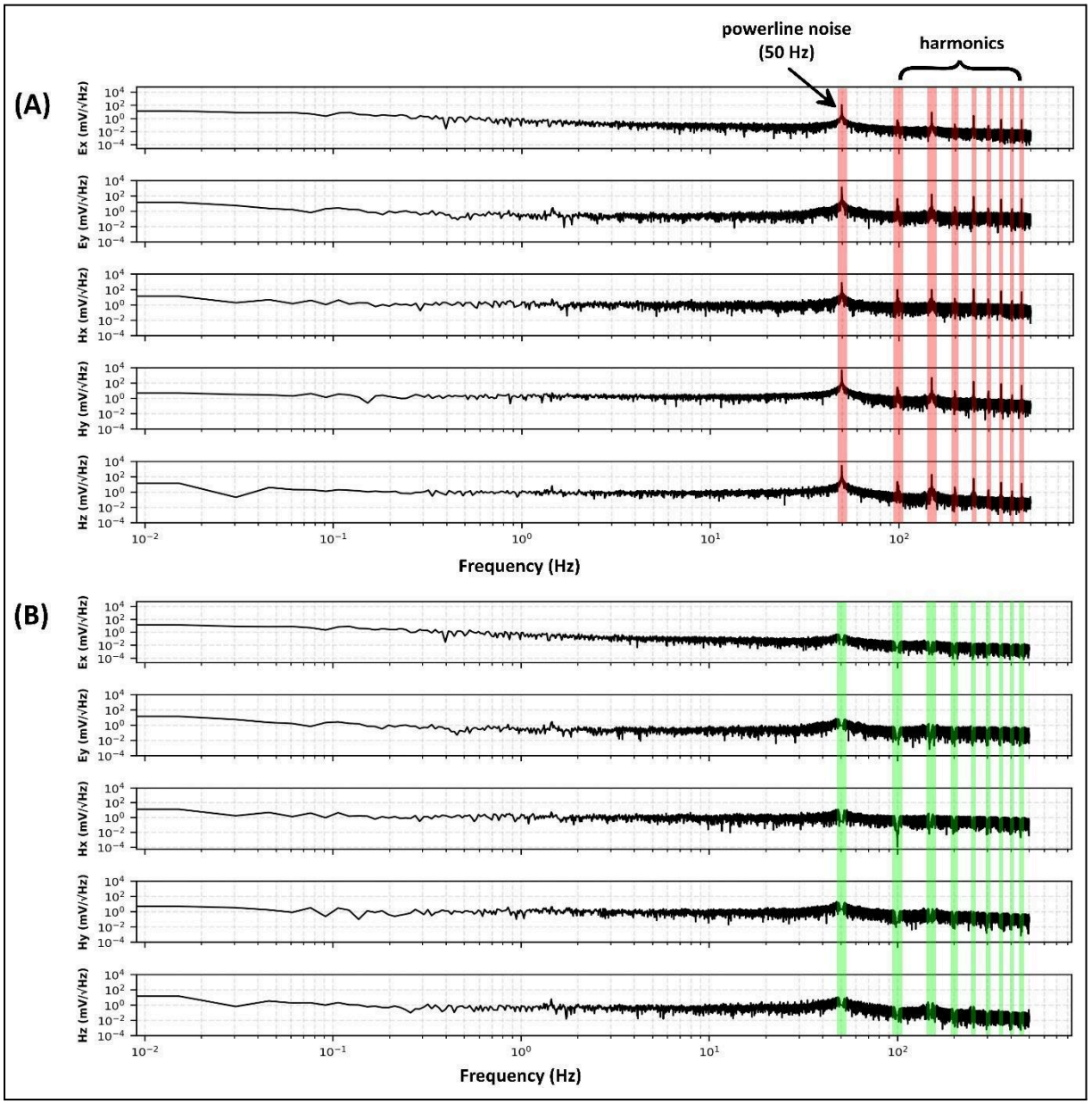



**Figure 6.** Data conditions when applying a notch filter. (a) Before; (b) After

The apparent resistivity and phase to frequency data result from a complex magnetotelluric transfer function process based on (1). This data can be categorized into xy data, which is owned as TE (transverse electric) mode, and yx data or TM (transverse magnetic) mode. In TE mode, the data measured in the field has an electric field orientation parallel to the strike assumption direction and a magnetic field perpendicular to the strike assumption direction. Meanwhile, the TM mode is the opposite, where the electric field is perpendicular to the

Copyright © 2026 Universitas Sebelas Maret

assumed strike direction and the magnetic field is parallel to the assumed strike direction. The apparent resistivity and phase data (Figure 7) can qualitatively represent the response of the subsurface conditions in the study area. High frequencies generally represent the response to shallow depths, while low frequencies represent the response to deep depths.

The qualitative analysis of phase data is based on [5], which explains that in the case of 1D magnetotellurics, a phase above 45° indicates a conductor. A phase below 45° reflects a resistor at a certain depth. The phase data obtained in this study can also explain this; Figure 7 shows that at shallow depths, phase values above 45° reflect a conductive anomaly, while at deep depths, phase values below 45° represent a resistive anomaly contrast. The presence of conductive anomalies in the study area can be explained through another approach, namely by analyzing tipper vector data, which is a complex geomagnetic transfer function obtained based on (4). This analysis is based on the induction arrows shown in Figure 7. The induction arrow convention (real part) used in this study is the Parkinson convention [30], where the magnitude of the induction arrow points toward the conductor. Figure 7 shows that the uniform magnitude of the induction arrow is visible in the frequency range of 2 Hz to 66 Hz, indicating the presence of a conductive medium at a relatively shallow depth.

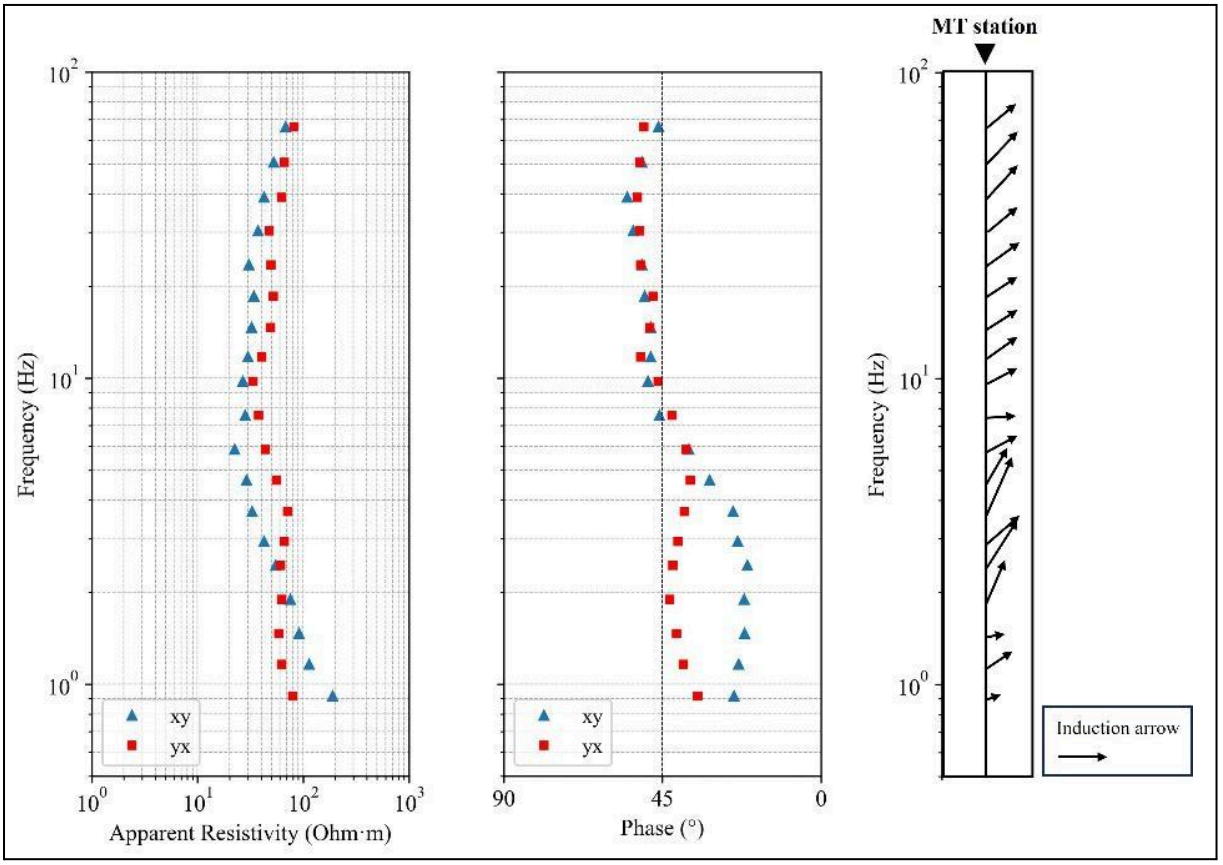



**Figure 7.** Apparent resistivity, phase, and tipper vector response in the frequency range of 0.9 – 66.4 Hz

Based on the results of qualitative analysis, MT data shows that the initial subsurface conditions in the measurement area generally consist of the conductive medium, which, based on regional geology, is alluvium, with a resistive medium underneath. This data is suitable for 1D magnetotelluric modeling to obtain variations in rock resistivity at certain depths.

To obtain a 1D resistivity model from magnetotelluric data measured in the field, 1D

Copyright © 2026 Universitas Sebelas Maret

inversion-based data modeling is carried out through IPI2WIN MT software. This software uses the Newton algorithm and Tikhonov regularization to solve the inversion problem and obtain a 1D resistivity model [39]. The input data required to run the inversion process in this study are frequency data, apparent resistivity, and phase in TE mode. The reason for choosing input data in TE mode is that it is more sensitive to conductive medium than TM mode [40], so it is suitable for modeling conductive alluvium layers. The 1D resistivity model resulting from the inversion process obtained in this study reaches a depth of up to 1000 m, as shown in Figure 8. The misfit of 7.4% can be categorized as a low misfit value, so the model obtained is consistent with the observation data.

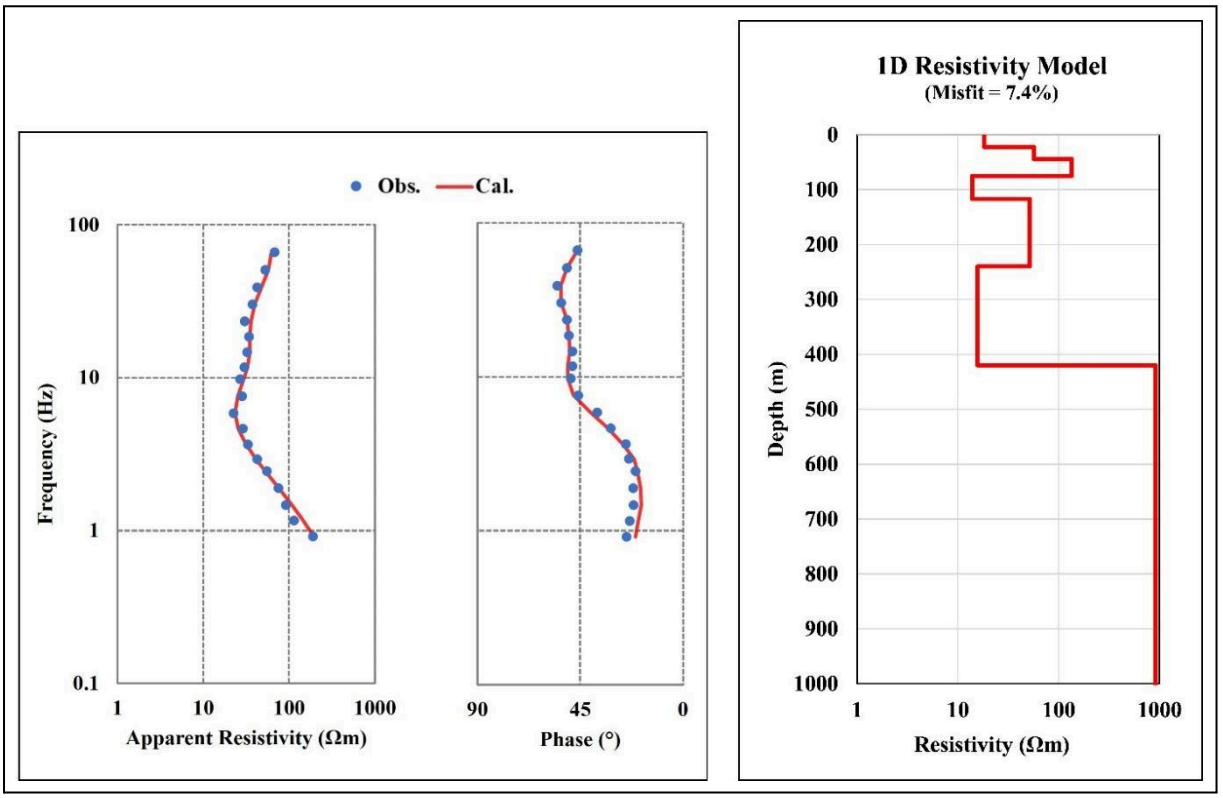



**Figure 8.** Result of 1D inversion modeling

The 1D resistivity model obtained from the inversion process shows seven subsurface layers to a depth of 1000 m in the study area, as shown in Table 2 and Figure 9. The resistivity values obtained vary from 13.9 Ωm to 914.22 Ωm. The resistivity value of 18.19 Ωm for the top layer at depths from 0 m to 22 m is interpreted as clay. In sequence, the second and third layers have resistivity values of 56.66 Ωm and 134.86 Ωm, interpreted as sand and gravel at depths of 22 m to 44 m and 44 m to 75 m, respectively. The next layer at a depth of 75 m to 117 m has a reduced resistivity value of 13.90 Ωm, interpreted as clay. The fifth layer at a depth of 117 m to 240 m and the sixth layer at a depth of 240 m to 420 m are interpreted as sand and clay with resistivity values of 51.80 Ωm and 15.66 Ωm, respectively. Layers one through six, consisting of clay, sand, and gravel, are believed to be the constituent materials of the alluvium formation in the Aceh River Delta. Meanwhile, the seventh, lowest layer shows a significant resistivity contrast of 914.22 Ωm. This layer is suspected to be filled with sandstone to conglomerate, which likely formed during the Tertiary period. Sedimentary rocks formed during this period have undergone compaction and lithification, resulting in high resistivity values [41]. A similar range of resistivity values (20–150 Ωm) characterizing layered clay–sand deposits has been reported from the Mekong Delta, Vietnam, where a

Copyright © 2026 Universitas Sebelas Maret

combined vertical electrical sounding (VES) and MT survey identified alluvium sediments overlying a highly resistive bedrock (10000 Ωm) [42].

**Table 2.** The 1D resistivity model interpretation results

| Layers | Resistivity (Ωm) | Depth (m) | Thickness (m) | Lithology Interpretation |
|---|---|---|---|---|
| 1 | 18.19 | 0 – 22 | 22 | Clay |
| 2 | 56.66 | 22 – 44 | 22 | Sand |
| 3 | 134.86 | 44 – 75 | 31 | Gravel |
| 4 | 13.90 | 75 – 117 | 42 | Clay |
| 5 | 51.80 | 117 – 240 | 123 | Sand |
| 6 | 15.66 | 240 – 420 | 180 | Clay |
| 7 | 914.22 | 420 – 1000 | 580 | Sandstone-conglomerate |

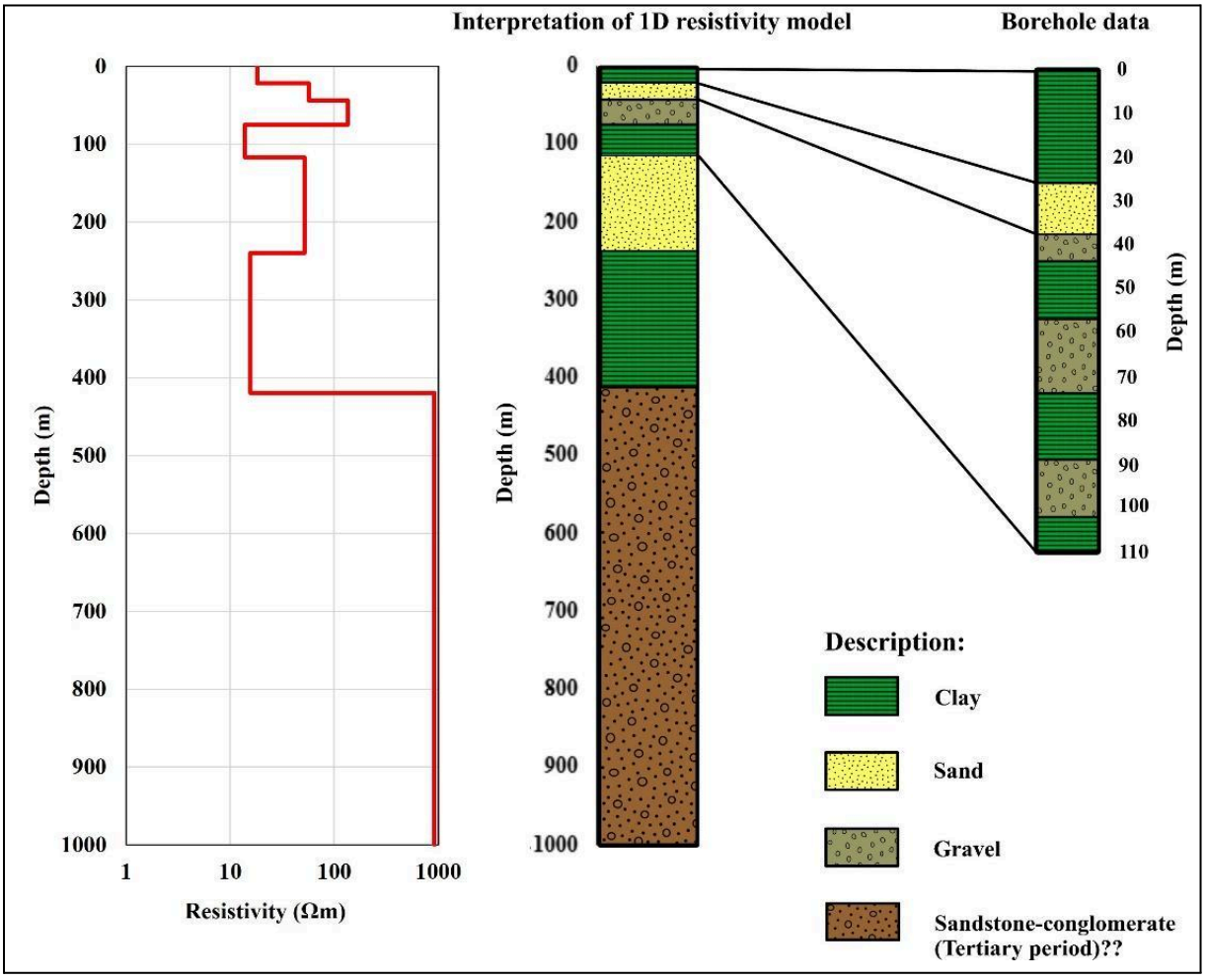



**Figure 9.** Lithological interpretation based on a 1D resistivity model correlated with borehole data [1]

The correlation between the 1D resistivity model interpretation results and geological data in the measurement area is necessary to evaluate the model's accuracy. In this study, the geological data obtained were borehole data taken from previous research [1]. These borehole data have a depth of 110 m and are located approximately 400 m from the magnetotelluric

Copyright © 2026 Universitas Sebelas Maret

data acquisition point. Based on Figure 9, it can be seen that the results of the 1D resistivity model interpretation have a good correlation with the borehole data, where the clay layer, which is the first layer of the model interpretation results, correlates with the clay layer from the borehole data located at a depth of 0 m to 25 m. The sand layer in the second layer of the model interpretation results correlates with the sand layer from the borehole data at 25 m to 38 m depth. Meanwhile, the gravel and clay layers in the third and fourth layers of the model interpretation results correlate with the mixed layer of gravel and clay from the borehole data at 38 m to 110 m depth. Therefore, the 1D resistivity model is quite accurate and represents the subsurface conditions in the study area well. A similar match between the 1D MT model and borehole data was also reported in the Kachchh Basin, India, where the layered model resulting from 1D inversion was consistent with the ONGC (Nirona) borehole data [12].

The estimated thickness of the alluvium in the study area is based on the 1D resistivity model interpretation results described earlier. Based on the range of resistivity values obtained from the model, clay material has a resistivity range of 13.9 Ωm to 18.2 Ωm, while sand-gravel material has a resistivity range of 51.80 Ωm to 134.86 Ωm. The resistivity values of clay, sand, and gravel obtained from the model are within the alluvium resistivity value range of 10 Ωm to 800 Ωm [43]. Meanwhile, the resistivity value of the sandstone-conglomerate obtained from the model is more than 900 Ωm. Clay, sand, and gravel lithology are unconsolidated sedimentary materials that form alluvium, as evidenced by their resistivity values. Meanwhile, sandstone-conglomerate is a sedimentary rock that has undergone lithification, resulting in a relatively high resistivity value that falls outside the alluvium resistivity range. Therefore, the subsurface geological conditions of the study area can be simplified into two layers: the alluvium formation at a depth of 0 m to 420 m with a thickness of 420 m, formed during the Quaternary period, and the sandstone-conglomerate formation at a depth of 420 m to 1000 m with a thickness of 580 m, which is suspected to have formed during the Tertiary period.

The successful application of the 1D MT method in estimating the thickness of alluvium to a depth of 420 m shows that this method effectively identifies the boundary between unconsolidated young sediment layers and older bedrock. The significant thickness of alluvium sediments increases the risk of earthquakes in the study area. Thick alluvium sediments tend to have low seismic wave propagation velocities and high amplification properties, thereby amplifying seismic waves propagating on the ground and potentially damaging infrastructures [44]. This relationship between low-resistivity sediment layers and high seismic amplification was also demonstrated in the 2006 Yogyakarta earthquake area, where AMT data identified soft layers with resistivity values of 5–70 Ωm (particularly 5–20 Ωm at depths of 0–500 m) corresponding to zones of severe surface damage [45]. Therefore, this study's findings are very useful in assessing earthquake risk. However, there are limitations in this study, namely that the 1D MT method can only model subsurface structures vertically at a single site, so lateral variations in alluvium thickness in the Aceh River Delta region have not been fully characterized. Therefore, to obtain a more comprehensive image of the distribution and thickness of alluvium across the entire study area, additional MT survey points are needed at strategic locations so that two-dimensional (2D) or three-dimensional (3D) modeling with higher resolution can be conducted in subsequent research.

## CONCLUSION

The 1D magnetotelluric method in the Aceh River Delta successfully identified Quaternary alluvium formations with low to moderate resistivity (13.9–134.9 Ωm), reaching a

Copyright © 2026 Universitas Sebelas Maret

cumulative thickness of up to ±420 m. This formation lies above a Tertiary bedrock with high resistivity (914.2 Ωm), interpreted as sandstone-conglomerate. The 1D resistivity model shows good correspondence with borehole lithology, supporting the reliability of the MT method in estimating alluvium thickness. The findings of this study indicate a significant accumulation of young sediments (alluvium). This information is important for earthquake risk assessment. Although the 1D resistivity model provides reliable results, further investigation using a dense MT array and 2D/3D inversion is recommended to reveal more comprehensive subsurface information, thereby enhancing geohazard assessment in the Aceh River Delta.

## ACKNOWLEDGMENTS

The authors would like to thank Wahyu Sandriadi, Muharrir Mutiara, Nur Jalal, Muhammad Farhan, and the data acquisition team. The authors would like to thank LPPM USK for funding this research through the Penelitian Professor (PP) grant, with contract number: 129/UN11.2.1/PG.01.03/SPK/PTNBH/2024.

## REFERENCES

[1] Rusydy, I., Ikhlas, Setiawan, B., Zainal, M., Idris, S., Basyar, K., & Putra, Y. A. 2020. Integration of borehole and vertical electrical sounding data to characterize the sedimentation process and groundwater in Krueng Aceh Basin, Indonesia. *Groundwater for Sustainable Development*, *10*(7), 100372–100383.

[2] Tohari, A., Sugianti, K., Syahbana, A. J., & Soebowo, E. 2015. Cone penetration test (CPT)-based liquefaction susceptibility of Banda Aceh City. *Jurnal Riset Geologi dan Pertambangan*, *25*(2), 99–110.

[3] Rusydy, I., Idris, Y., Muksin, U., Cummins, P., Akram, M. N., & Syamsidik. 2020. Shallow crustal earthquake models, damage, and loss predictions in Banda Aceh, Indonesia. *Geoenvironmental Disasters*, *7*(1), 1–16.

[4] Cagniard, L. 1953. Basic theory of the magneto‐telluric method of geophysical prospecting. *Geophysics*, *18*(3), 605–635.

[5] Vozoff, K. 1991. The magnetotelluric method. In M. N. Nabighian & J. D. Corbett (Eds.), *Electromagnetic methods in applied geophysics: Volume 2, application, parts A and B* (pp. 641–711). Society of Exploration Geophysicists.

[6] Sarvandani, M. M., Kalateh, A. N., Unsworth, M., & Majidi, A. 2017. Interpretation of magnetotelluric data from the Gachsaran oil field using sharp boundary inversion. *Journal of Petroleum Science and Engineering*, *149*(1), 25–39.

[7] Aboud, E., Hamed, T. A., Alqahtani, F., Marzouk, H., Elbarbary, S., Abdulfaraj, M., & Elmasry, N. 2023. The geothermal magmatic system at the northern Rahat volcanic field, Saudi Arabia, revealed from 3D magnetotelluric inversion. *Journal of Volcanology and Geothermal Research*, *437*(1).

[8] Ismail, N., Schwarz, G., & Pedersen, L. B. 2011. Investigation of groundwater resources using controlled-source radio magnetotellurics (CSRMT) in glacial deposits in Heby, Sweden. *Journal of Applied Geophysics*, *73*(1), 74–83.

[9] Jiang, W., Duan, J., Doublier, M., Clark, A., Schofield, A., Brodie, R. C., & Goodwin, J. 2022. Application of multiscale magnetotelluric data to mineral exploration: An example from the east Tennant region, Northern Australia. *Geophysical Journal International*, *229*(3), 1628–1645.

[10] Tournerie, B., & Chouteau, M. 2005. Three-dimensional magnetotelluric survey to image structure and stratigraphy of a sedimentary basin in Hungary. *Physics of the Earth and Planetary Interiors*, *150*(1–3), 197–212.

[11] Yin, Y., Jin, S., Wei, W., Lü, Q., Ye, G., Jing, J., Zhang, L., Dong, H., & Xie, C. 2021. Lithosphere structure and its implications for the metallogenesis of the Nanling Range, South China: Constraints from 3-D magnetotelluric imaging. *Ore Geology Reviews*, *131*.

Copyright © 2026 Universitas Sebelas Maret

[12] Patel, P., Mohan, K., & Chaudhary, P. 2020. Estimation of sediment thickness (including Mesozoic) in the western central part of Kachchh Basin, Gujarat (India) using magnetotellurics. *Journal of Applied Geophysics*, *173*, 103943–103958.
[13] Dhamodharan, S., Rawat, G., Kumar, S., & Bagri, D. S. 2020. Sedimentary thickness of the northern Indo-Gangetic plain inferred from magnetotelluric studies. *Journal of Earth System Science*, *129*(1), 1–12.
[14] Adilakshmi, L., Manglik, A., Thiagarajan, S., & Suresh, M. 2021. Crustal structure of the Indian plate underneath the alluvial plains of the central Ganga basin by broadband magnetotellurics. *Tectonophysics*, *802*(1), 228746–228759.
[15] Siemon, B., & Steuer, A. 2010. Airborne geophysical investigation of groundwater resources in Northern Sumatra after the tsunami of 2004. In *Tsunami Threat – Research and Technology*.
[16] Polom, U., Arsyad, I., & Kümpel, H. J. 2008. Shallow shear-wave reflection seismics in the tsunami-struck Krueng Aceh River Basin, Sumatra. *Advances in Geosciences*, *14*, 135–140.
[17] Rizal, M., Ismail, N., Yanis, M., Muzakir, & Surbakti, M. S. 2019. The 2D resistivity modelling on North Sumatran fault structure by using magnetotelluric data. *IOP Conference Series: Earth and Environmental Science*, *364*(1).
[18] Roodhiyah, L. Y., Nurhasan, Tiffany, Pratomo, P. M., Susilawati, A., Supriadi, Ogawa, Y., Sugiyanto, D., Sutarno, D., & Srigutomo, W. 2024. Interpretation of a 3D magnetotellurics model of the Aceh and Seulimeum Segments of the Sumatran Fault Zone. *Applied Sciences*, *14*(23).
[19] Marwan, Yanis, M., Zahratunnisa, Idroes, R., Nugraha, G. S., Dharma, D. B., Susilo, A., Saputra, D., Suriadi, & Paembonan, A. Y. 2022. Geothermal reservoir depth of Seulawah Agam Volcano estimated from 1D magnetotelluric. *Journal of Applied Engineering Science*, *20*(3), 754–764.
[20] Marwan, M., Yanis, M., Nugraha, G. S., Zainal, M., Arahman, N., Idroes, R., Dharma, D. B., Saputra, D., & Gunawan, P. 2021. Mapping of fault and hydrothermal system beneath the Seulawah volcano inferred from a magnetotellurics structure. *Energies*, *14*(19), 1–22.
[21] Bennett, J. D., Bridge, D. McC., Cameron, N. R., Djunuddin, A., Ghazali, S. A., Jeffery, D. H., Kartawa, W., Keats, W., Rock, N. M. S., Thompson, S. J., & Whandoyo, R. 1981. *Geologic map of the Banda Aceh quadrangle, Sumatra*.
[22] Culshaw, M. G., Duncan, S. V., & Sutarto, N. R. 1979. Engineering geological mapping of the Banda Aceh alluvial basin, Northern Sumatra, Indonesia. *Bulletin of the International Association of Engineering Geology*, *19*(1), 40–47.
[23] Chapkanski, S., Doaré, M. L., Brocard, G., Steuer, A., Siemon, B., Lavigne, F., Ismail, N., Meilianda, E., Viermoux, C., Darusman, & Goiran, J. P. 2023. Distribution of landforms and buried sedimentary deposits during the growth of the Aceh River delta (Sumatra, Indonesia). *Journal of Maps*, *19*(1), 1–15.
[24] Sieh, K. & Natawidjaja, D. 2000. Neotectonics of the Sumatran fault, Indonesia. *Journal of Geophysical Research: Solid Earth*, *105*(B12), 28295–28326.
[25] Jihad, A., Banyunegoro, V. H., Umar, M., Ramli, M., Syamsidik, Idris, Y., & Rusdin, A. A. 2024. Characterizing earthquake source parameters and b-value variations in subduction and fault segments: Implications for seismic hazard analysis. *Journal of Mathematics in Fundamental Sciences*, *56*(1), 1–17.
[26] Asnawi, Y., Simanjuntak, A. V. H., Umar, M., Rizal, S., & Syukri, M. 2020. A microtremor survey to identify seismic vulnerability around Banda Aceh using HVSR analysis. *Elkawnie*, *6*(2), 342–358.
[27] Baker, W. G., & Martyn, D. F. 1953. Electric currents in the ionosphere – the conductivity. *Philosophical Transactions of the Royal Society of London. Series A, Mathematical and Physical Sciences*, *246*(913), 281–294.
[28] Bonner, L. R., & Schultz, A. 2017. Rapid prediction of electric fields associated with geomagnetically induced currents in the presence of three-dimensional ground structure: Projection of remote magnetic observatory data through magnetotelluric impedance tensors. *Space Weather*, *15*(1), 204–277.
[29] Simpson, F., & Bahr, K. 2005. Basic theoretical concepts. In *Practical Magnetotellurics* (1st

Copyright © 2026 Universitas Sebelas Maret

ed.). Cambridge University Press.
[30] Parkinson, W. D. 1962. The influence of continents and oceans on geomagnetic variations. *Geophysical Journal of the Royal Astronomical Society*, *6*(4), 441–449.
[31] Haaf, N., & Schill, E. 2021. Noise during long-term continuous magnetotelluric monitoring of RN-15/IDDP-2 well engineering (Reykjanes Peninsular, Iceland): A geogenic origin?. *Geothermics*, *96*.
[32] Egbert, G. D., & Eisel, M. 1997. EMTF: Programs for robust single station and remote reference analysis of magnetotelluric data. Oregon State University.
[33] Roy, K. K. 2020. Magnetotellurics. In *Natural Electromagnetic Fields in Pure and Applied Geophysics* (1st ed.). Cham: Springer International Publishing.
[34] Zhan, Q., Liu, C., Liu, Y., & Zhao, P. 2023. Data processing method for magnetotelluric sounding based on cepstral analysis. *Frontiers in Earth Science*, *11*(1), 1–15.
[35] Wang, H., Campanyà, J., Cheng, J., Zhu, G., Wei, W., Jin, S., & Ye, G. 2017. Synthesis of natural electric and magnetic time-series using inter-station transfer functions and time-series from a neighboring site (STIN): Applications for processing MT data. *Journal of Geophysical Research: Solid Earth*, *122*(8), 5835–5851.
[36] Jeon, H., Jung, Y., Lee, S., & Jung, Y. 2020. Area-efficient short-time Fourier transform processor for time–frequency analysis of non-stationary signals. *Applied Sciences*, *10*(20), 1–10.
[37] Fontes, S. L., Harinarayana, T., Dawes, G. J. K., & Hutton, V. R. S. 1988. Processing of noisy magnetotelluric data using digital filters and additional data selection criteria. *Physics of the Earth and Planetary Interiors*, *52*(1–2), 30–40.
[38] Sulaiman, F. A., Ismail, M. L., & Daud, Y. 2021. Processing of noise-contaminated magnetotelluric data using digital filters based on MATLAB. *Journal of Physics: Conference Series*, *1725*(1).
[39] Bobachev, A. A. 2002. *IPI2Win(MT) v. 2.0 User's Guide*. Moscow State University.
[40] Kalscheuer, T., Juhojuntti, N., & Vaittinen, K. 2018. Two-dimensional magnetotelluric modelling of ore deposits: Improvements in model constraints by inclusion of borehole measurements. *Surveys in Geophysics*, *39*(3), 467–507.
[41] Palacky, G. J. 1987. Resistivity characteristics of geologic targets. In M. N. Nabighian & J. D. Corbett (Eds.), *Electromagnetic methods in applied geophysics: Volume 1, theory* (pp. 53–129). Society of Exploration Geophysicists.
[42] Van, G. N., Trong, V. N., & Huy, V. N. 2023. Groundwater Investigation by Combined Vertical Electrical Sounding and Magnetotelluric Sounding in Eastern Region of Mekong Delta, in the South of Vietnam. *Binh Duong University Journal of Science and Technology*, *5*(4).
[43] Reynolds, J. M. 2011. *An introduction to applied and environmental geophysics* (2nd ed.). Wiley-Blackwell.
[44] Sundararajan, N., & Seshunarayana, T. 2018. Shear wave velocities in the estimation of earthquake hazard over alluvium in seismically active region. *Journal of the Geological Society of India*, *92*(3), 259–264.
[45] Nurhasan, Risky, N. D. S., Pratama, A., Zahra, I., & Ogawa, Y. 2024. Analysis of subsurface Resistivity Structures in Relation to the Level of Damage Caused by Earthquakes Using the Audio-Magnetotelluric (AMT) Method (Case study: The 2006 Yogyakarta Earthquake). *Journal of Physics: Conference Series*, *2866*(1).

Copyright © 2026 Universitas Sebelas Maret